Spectrochimica Acta Part A: Molecular and Biomolecular Spectroscopy 278 (2022) 121334

Contents lists available at ScienceDirect

Spectrochimica Acta Part A: Molecular and Biomolecular Spectroscopy

journal homepage: www.elsevier.com/locate/saa

A new six-membered spiro-rhodamine probe for Cu^{2+} and its imaging in mitochondria and lysosomes of Hela cells

Yongsheng Lei [a], Yannan Xiao [a], Lin Yuan [a], Chen Ma [a], Haibo Yu [a,b,*], Xinfu Zhang [b,*], Ying Zhang [a,*], Yi Xiao [b]

[a] College of Environmental Sciences, Liaoning University, Shenyang 110036, PR China
[b] State Key Laboratory of Fine Chemicals, Dalian University of Technology, Dalian 116024, PR China

HIGHLIGHTS

- A new six-membered spiro-rhodamine probe was designed and synthesized.
- Molar extinction coefficient of SRh-OH with Cu^{2+} can be up to 5.0×10^4 $Lmol^{-1}cm^{-1}$.
- The detection limit of SRh-OH was 26 nM.
- The reversible binding mode of SRh-OH with Cu^{2+} was further confirmed by S^{2-} addition.
- SRh-OH can map the distribution of Cu^{2+} in mitochondria and lysosomes, simultaneously.

GRAPHICAL ABSTRACT

A new six-membered spiro-rhodamine probe with high selectivity and sensitivity for Cu^{2+} has been developed and used to map the distribution of Cu^{2+} in mitochondria and lysosomes simultaneously of live Hela cells.

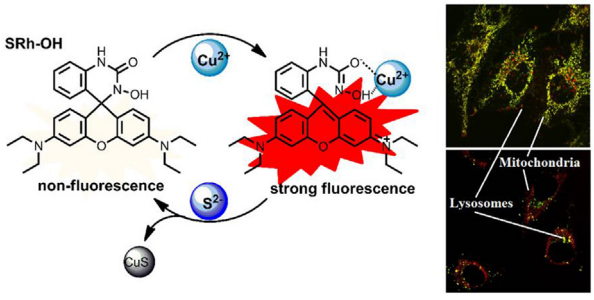

ARTICLE INFO

Article history:
Received 21 December 2021
Received in revised form 6 April 2022
Accepted 28 April 2022
Available online 4 May 2022

Keywords:
Six-membered
Cu^{2+} monitoring
Rhodamine
Mitochondrion and lysosomes-targetable
Fluorescent imaging

ABSTRACT

Different from five-membered rhodamine spirolactam (Rh-OH), a new six-membered spiro-rhodamine probe (SRh-OH) bearing urea structure has been developed in this paper. Compared with five-membered Rh-OH, six-membered SRh-OH exhibited higher selectivity and sensitivity to Cu^{2+} in aqueous solution. Upon addition of 10 equiv. Cu^{2+}, the molar extinction coefficient of SRh-OH at 563 nm can be up to 4.73×10^4 $Lmol^{-1}cm^{-1}$. In the range of Cu^{2+} from 0 to 28 μM, there was an excellent linear relationship between the absorption or emission intensity and Cu^{2+} concentration. The detection limit of SRh-OH was as low as 26 nM (S/N = 3). The reversible binding mode of SRh-OH with Cu^{2+} was further confirmed by S^{2-} and EDTA addition. Bio-imaging showed SRh-OH can map the distribution of Cu^{2+} not only in mitochondria but also in lysosomes of Hela cells.

1. Introduction

Attributing to its excellent optical properties such as high fluorescent quantum yield and molar extinction coefficient, rhodamine has been widely used in the fields of fluorescent sensors [1–4], printing and dyeing [5,6], thermosensitive materials [7,8], optoelectronic devices [9,10], super-resolution imaging [11–13], and so on. Rhodamine spirolactam bearing five-membered moiety was one of the most familiar rhodamine derivatives as fluorescent probe [14–19]. The "off–on" fluorescence derived from ring-switch of these rhodamine spirolactams provided low background and high signal-to-noise ratio for sensing. A cruel fact should not be ignored, that the ring-opening tendency of rhodamine spirolactam induced by analytes was not very efficient, leading to low molar extinction coefficient. To this end, a lot of work focused on the modification of primary amine moiety in rhodamine spirolactam

* Corresponding authors.
E-mail addresses: yuhaibo@lnu.edu.cn (H. Yu), zhangxinfu@dlut.edu.cn (X. Zhang), yingying0809@126.com (Y. Zhang).

https://doi.org/10.1016/j.saa.2022.121334
1386-1425/

has been reported to increase its selectivity and sensitivity to some degree [20–23]. However, that method with a high difficulty level in the synthesis of primary amine moiety was not always universal for other analytes.

Compared with rhodamine spirolactam, the expansion of spirocycle would be an opportunity for selectivity, sensitivity and high molar extinction coefficient once and for all. Several six-membered rhodamine spirocycles have been reported and utilized in the detection of metal ions including Hg^{2+} and Cu^{2+} [24–29]. Expansion of spiocycle in rhodamine also excited our interest. Recently, we firstly designed a twist six-membered rhodamine spirocyclic hydrazone(6G-ClO) for hypochlorite detection, based on 2-aldehyde rhodamine(6G-CHO) [30]. The twist six-membered structure played a vital role in the sensitivity to hypochlorite. But the expansion of spirocycle being helpful to the selectivity and sensitivity for analytes was not directly expounded by the reported six-membered rhodamine spirocycles. Therefore, clearly elaborating the relationship between properties and ring size of spirocycle was highly meaningful yet challenging.

No doubt the key problems above-mentioned were to establish a universal synthetic route and develop much more six-membered rhodamine spirocycles. Herein, we put forward a general synthetic route to develop a new six-membered rhodamine spirocycle (SRh-OH) bearing with urea structure, and further compared its properties for Cu^{2+} with a reference five-membered spirolactam (Rh-OH) (Scheme 1). Rh-OH used as a Cu^{2+} probe has highly selective and sensitive fluorescence response in acidic solution with pH value around 6.0 [31].

2. Experiment

2.1. Materials and methods

All regents, e.g. $ClCH_2CH_2Cl$, $POCl_3$, NaN_3, acetonitrile, triethylamine, etc., were purchased from commercial suppliers and used as received without further purification. Rh-OH was obtained according to the reported method in literature [31]. Thin layer chromatography (TLC) was performed using silica gel G254 plates. Flash chromatography was carried out on silica gel (300–400 mesh). Mass spectra were measured on a HP 1100 LC-MSD, Gas chromatography/TOF Mass spectrometers and the UPLC/Q-TOF Mass spectrometers. A PHS-25 desktop pH-meter was used to measure pH value. UV–Visible spectra were recorded on a TU-1910 spectrophotometer. Cary Eclipse spectrophotometer was used to record the fluorescence spectra. ^1H and ^{13}C NMR spectra were recorded on a Varian MERCURY 500 MHz spectrometer. IR data was obtained from IS50 FT-IR (Thermo Nicolet). An inverted confocal fluorescent microscopy (IX81, FV1000, Olympus, Japan) equipped with an objective lens (×100 oil, 1.4 Numerical Aperture (NA), Scan mode XY) was used in the imaging of living cells.

2.2. Synthesis of SRh-OH

Rhodamine B (300 mg, 0.6 mmol) and phosphorus oxychloride (0.18 mL, 1.8 mmol) were dissolved in 100 mL dry 1,2-dichloroethane, and the mixture was heated at 90 °C for 4 h. The reaction was cooled to room temperature and the solvent was removed. The obtained solid was dissolved in 100 mL dry acetonitrile before sodium azide (51 mg, 0.78 mmol) in aqueous solution was added. The mixture was stirred at room temperature for 12 h. The resulting reaction solution was dried with anhydrous $MgSO_4$ and then filtered. The filtrate was heated at 82 °C for 60 min. The solution was cooled to room temperature and a DMF solution containing hydroxylamine (0.0417 g, 0.6 mmol) and triethylamine (84 μL, 0.6 mmol) was added. The reaction was stirred at room temperature for 1 h before the solvent was removed. White solid SRh-OH (32 mg) was purified by column chromatography (CH_2Cl_2: MeOH, 30: 1, v:v), and the total yield was about 11%. HRMS: $[M + H]^+$ 473.2533, cal. 473.2553, ^1H NMR (400 MHz, $CDCl_3$) δ 8.18 (s, 1H), 7.16–7.09 (m, 1H), 7.04 (dd, J = 9.8, 2.5 Hz, 2H), 6.87–6.76 (m, 3H), 6.41–6.33 (m, 4H), 3.33 (q, J = 7.0 Hz, 8H), 1.16 (tD, J = 7.0 Hz, 12H). ^{13}C NMR (100 MHz, $CDCl_3$) δ 153.2, 152.7, 148.7, 133.7, 129.9, 129.6, 128.2, 122.8, 114.1, 110.2, 108.1, 97.3, 65.3, 44.3, 12.7. FT-IR (KBr, cm^{-1}): 3223, 2975, 2926, 1671, 1613, 1510, 1419, 1221, 1117, 824, 787, 752.

2.3. Preparation of the test solutions and spectral measurements

SRh-OH (9.50 mg, 0.02 mmol) was dissolved in a aqueous solution (CH_3CN/HEPES buffer (v:v, 4:6, pH 7.4)) in 1000 mL volumetric flask. The concentration of test solution of SRh-OH was 2×10^{-5} M. The concentration of Cu^{2+}, other metal ion and anions was 2.0×10^{-2} M and used for selectivity and titration experiments. The UV–Visible absorption spectra and fluorescence spectra of

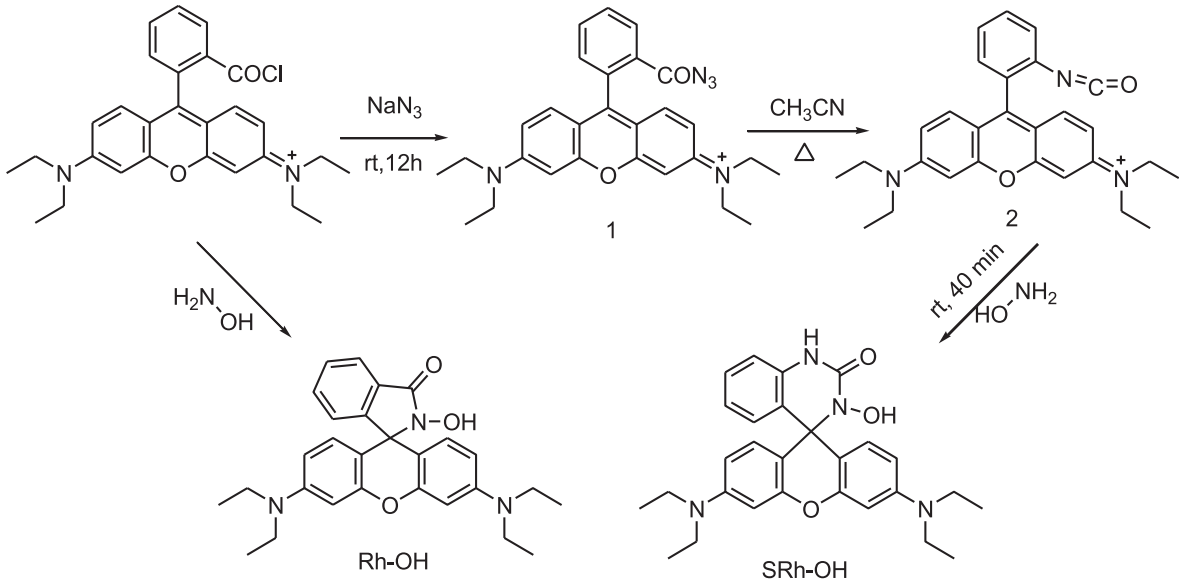

Scheme 1. The synthetic route of six-membered spirocycle (SRh-OH) and five-membered spirolactam (Rh-OH).

SRh-OH were recorded after a certain amount of analytes were added into the test solution.

2.4. Kinetic analysis of SRh-OH towards Cu^{2+}

Different concentrations Cu^{2+} were added into the solution of SRh-OH and Rh-OH, respectively. The fluorescent intensity at maximum emission peak of SRh-OH and Rh-OH towards Cu^{2+} were recorded on fluorescence spectrophotometer within 1 min.

2.5. pH adjustment

The pH values of SRh-OH and Rh-OH solution were adjusted from 2.0 to 11.0 by NaOH and HCl solution under magnetic stirring. The pH values of the solution were recorded on pH meter, and the absorption and emission spectra of SRh-OH and Rh-OH solution at different pH values were tested.

3. Results and discussion

3.1. Synthesis

To construct more six-membered rhodamine spirocycles, a universal one-pot three step synthetic process was developed (Scheme 1). The inexpensive 2-carboxyl rhodamine used as material successively reacted with phosphorus oxychloride and sodium azide to generate 2-acyl azide rhodamine. The reaction mixtures were heated at 82 °C to produce 2-isocyanate rhodamine. Then new six-membered rhodamine spirocycle SRh-OH can be obtained with 11% total yield. Different from 2-isothiocyanate rhodmaine, 2-isocyanate rhodamine can be easily obtained from 2-acyl azide rhodamine at high temperature. Toxic thiophosgene was used in the synthesis of 2-isothiocyanate rhodmaine based on 2-amino rhodamine [28]. Moreover, sulfur atom in 2-isothiocyanate usually exhibited a strong affinity to heavy metal ions such as Hg^{2+} and Cu^{2+}, which might be not conducive to its selectivity for other metal ions. Therefore, 2-isocyanate rhodamine could be used as a universal platform to design various six-membered rhodamine fluorescent probes.

3.2. pH responses of SRh-OH and Rh-OH

The spectral responses of SRh-OH and Rh-OH to pH were tested in CH_3CN/H_2O (4:6, v/v) solution, respectively (Fig. 1). At pH greater than 6.0, both SRh-OH and Rh-OH were colorless and its fluorescence was also not observed. With decreasing of pH value, a pink color of SRh-OH solution was visible, and an absorption peak at 563 nm could be detected. Meanwhile, the fluorescence intensity gradually increased at 593 nm. The absorption and emission spectra of SRh-OH and Rh-OH were compared at the same pH values (Fig. S1). Compared with SRh-OH, Rh-OH exhibited similar spectral responses in the pH range from 3.0 to 11.0. However, there was a large discrepancy between molar extinction coefficient and fluorescent intensity. In acidic conditions, SRh-OH has a higher molar extinction coefficient (4.95×10^3 $Lmol^{-1}cm^{-1}$) than that of Rh-OH (1.15×10^3 $Lmol^{-1}cm^{-1}$). The fluorescent intensity of SRh-OH was about three times as many as Rh-OH at pH 4.0. These results indicated the spectra of SRh-OH were more sensitive to pH in the range 3.0–6.0, compared with Rh-OH. The pKa value of SRh-OH was 5.06 (±0.14) (abs) and 4.92 (±0.31) (fl) respectively calculated by absorption and fluorescent titration spectra, similar to that of Rh-OH (4.80 (±0.60) (abs) and 4.95 (±0.08)) (fl). The weak absorption and fluorescence at pH above 7.0 further indicated that six-membered spirocycle in SRh-OH was as stable as five-memebered spirolactam, which would be suitable for metal ion probes.

3.3. Selectivity of SRh-OH for Cu^{2+}

The selectivity of SRh-OH to vary metal ions and anions were investigated in CH_3CN/HEPES (4:6, v/v, pH7.4) buffer solution. As shown in Fig. 2, the absorption and emission spectra did not change in the presence of 10 equiv. metal ions, such as Fe^{3+}, Fe^{2+}, Al^{3+}, Mg^{2+}, Na^{+}, Ca^{2+}, Hg^{2+}, K^{+}, Mn^{2+}, Cr^{3+}, Zn^{2+}, Pb^{2+} and Cd^{2+}. Upon addition of 10 equiv. Cu^{2+}, SRh-OH solution changed color from colorless to red. There was a new absorption peak at 563 nm and its molar extinction coefficient was up to 4.73×10^4 $Lmol^{-1}cm^{-1}$ (Fig. 2a). Meanwhile, a strong fluorescence arose at 593 nm upon excitation at 560 nm (Fig. 2b). Under the same conditions, five-membered spirolactam Rh-OH showed weak spectral responses to Cu^{2+} (Fig. S2). The molar extinction coefficient of Rh-OH was only 2.45×10^3 $Lmol^{-1}cm^{-1}$ in the presence of 10 equiv. Cu^{2+}, which suggested that there was a low ring-opening efficiency of Rh-OH induced by Cu^{2+}. In addition, the ring-opening transformation of SRh-OH was not significantly interfered by 10 equiv. metal ions and anions including NO_3^-, F^-, I^-, CO_3^{2-}, HPO_4^{2-}, $H_2PO_4^-$, S^{2-}, ClO^-, Cl^- and SO_4^{2-} (Fig. 2c, 2d and S3).

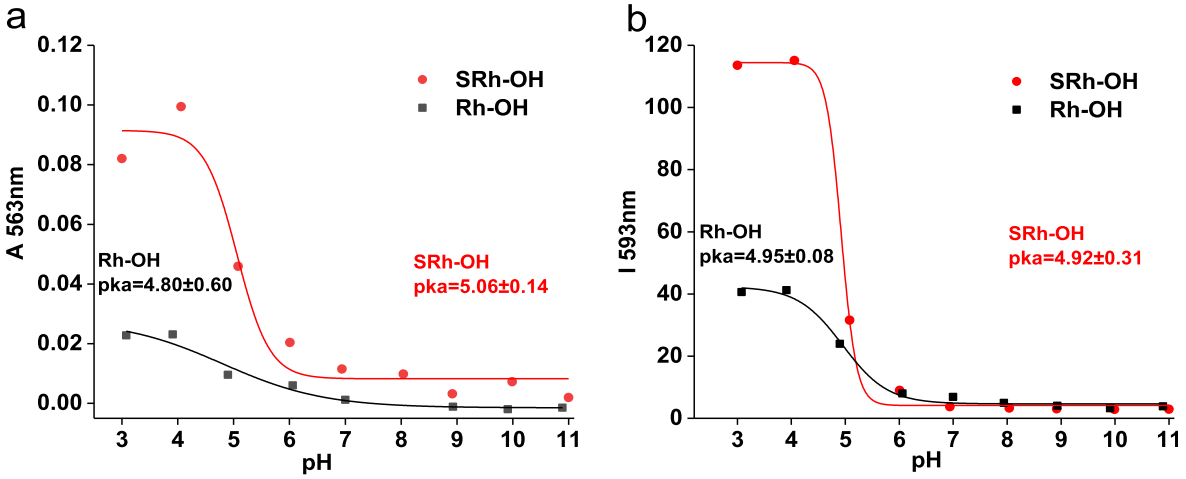

Fig. 1. The maximum of absorption (a) and emission (b) intensity of SRh-OH (red) and Rh-OH (black) in CH_3CN/H_2O (4:6, v/v) vs pH. (For interpretation of the references to color in this figure legend, the reader is referred to the web version of this article.)

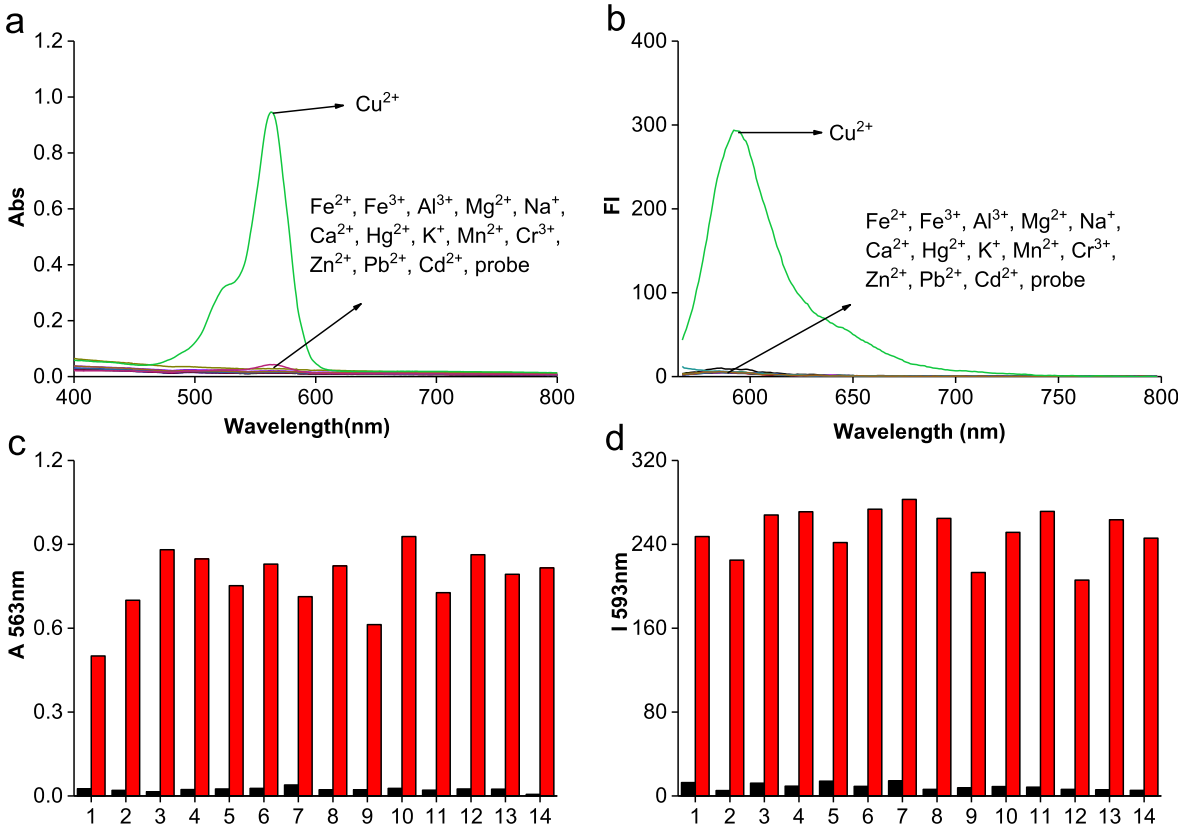

Fig. 2. Absorption (a) and emission (b) spectra of SRh-OH (CH_3CN/HEPES, v/v, 4/6, pH 7.4) in the presence of 10 equiv. metal ions. (c) Absorption intensity (563 nm) and (d) emission intensity (593 nm) of SRh-OH vs metal ions in the presence of Cu^{2+} ion (10 equiv). 1. Fe^{3+}, 2. Fe^{2+}, 3. Al^{3+}, 4. Mg^{2+}, 5. Na^{+}, 6. Ca^{2+}, 7. Hg^{2+}, 8. K^{+}, 9. Mn^{2+}, 10. Cr^{3+}, 11. Zn^{2+}, 12. Pb^{2+}, 13. Cd^{2+}, 14. Blank.

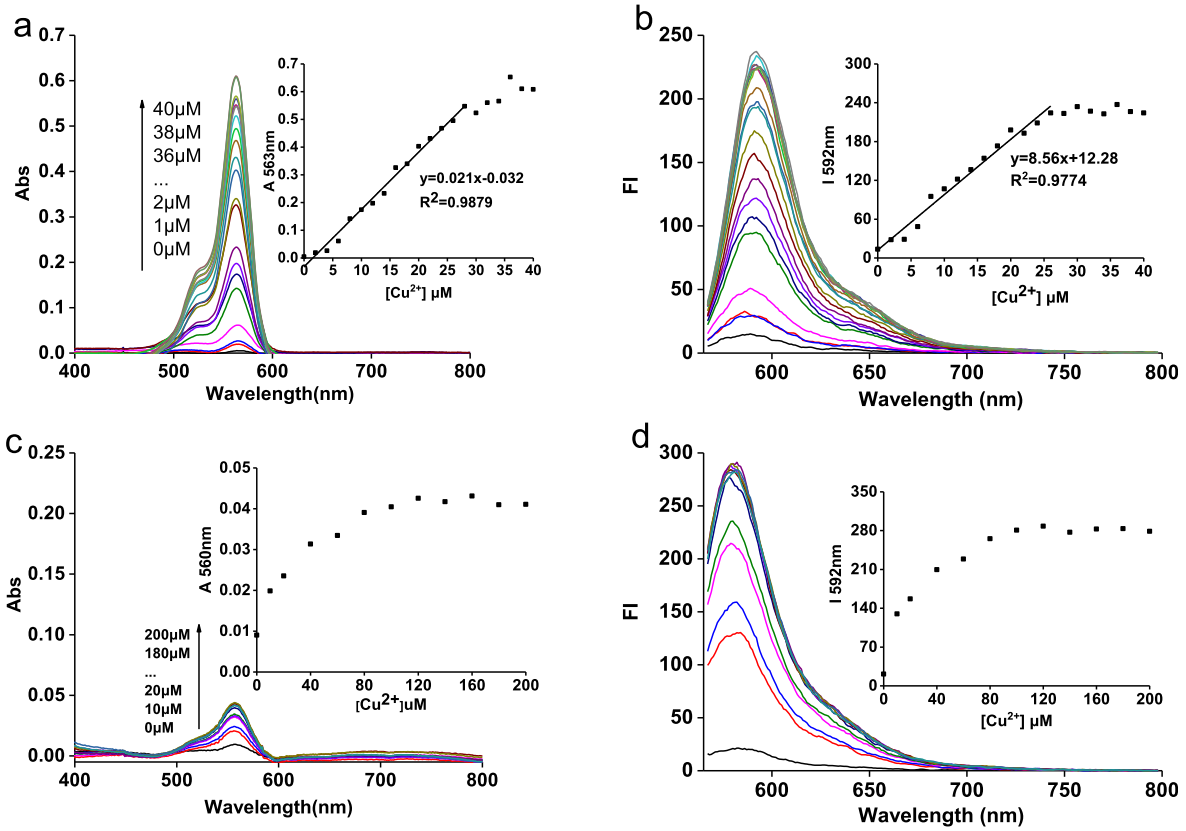

Fig. 3. Spectral changes of SRh-OH (2.0×10^{-5} M) (a-b) and Rh-OH (2.0×10^{-5} M) (c-d) in CH_3CN/HEPES (4/6, v/v, 20 mM HEPES buffer, pH 7.4) with addition of Cu^{2+}. Inset: the absorption and emission intensity versus the different concentration of Cu^{2+}. SRh-OH: λex 560 nm, slit: 2.5, 2.5 nm. Rh-OH: λex 560 nm, slit: 2.5, 5 nm.

3.4. Cu^{2+} titration

To compare the discrepancy on Cu^{2+} responses, titrations of SRh-OH and Rh-OH with Cu^{2+} were tested in CH_3CN/HEPES (4:6, v/v, pH 7.4). As shown in Fig. 3, the solution of SRh-OH was colorless and non-fluorescent in absence of Cu^{2+}, which meant that a closed six-membered spirocycle structure could stably exist in SRh-OH. With gradual addition of Cu^{2+}, the color of SRh-OH solution changed to bright pink following an intensive absorption peak at 563 nm (Fig. 3a). Simultaneously, a new fluorescence emission band centered at 592 nm appeared and increased gradually (Fig. 3b). The absorption titration curve showed that the absorption intensity at 563 nm increased linearly in the range of Cu^{2+} concentration from 0 to 28 μM (R^2 = 0.988). Compared with SRh-OH, five-membered spirolactam Rh-OH showed poor spectral responses to Cu^{2+} in CH_3CN/HEPES (4:6, v/v, pH 7.4). After addition of 120 μM Cu^{2+}, the color of Rh-OH solution became light pink, meanwhile, the maximum absorption intensity at 563 nm was only 0.043 (Fig. 3c). Upon addition of 28 μM Cu^{2+} into SRh-OH solution, the maximum absorption intensity could be up to 0.55. Accordingly, the fluorescent intensity of SRh-OH solution at 593 nm enhanced 17-folds. Calculated by the ratio of signal to noise(S/N = 3) [32], the detection limit of SRh-OH and Rh-OH were 26 nM and 548 nM, respectively. These results implied that SRh-OH might display a higher sensitivity for Cu^{2+} than Rh-OH.

3.5. Reversibility of SRh-OH with Cu^{2+}

The reversibility of SRh-OH with Cu^{2+} was examined in CH_3CN-HEPES (20 mM, 4:6, v:v, pH 7.4) buffer solution upon addition of EDTA or S^{2-}. As shown in Fig. 4, upon addition of 10 equiv. of Cu^{2+}, the absorption peak at 563 nm of SRh-OH solution was visible while the red fluorescence at 593 nm was significantly enhanced. Then the intensity of absorption and emission of SRh-OH decreased instantly after 10 equiv. EDTA was added. Subsequently, the recovery of absorption and emission intensity for SRh-OH added into 10 equiv. Cu^{2+} suggested a reversible response of SRh-OH to Cu^{2+} (Fig. 4a, 4b). Different from SRh-OH, mask of Cu^{2+} by EDTA did not decrease the intensity of absorption and fluorescence of Rh-OH and Cu^{2+} mixture (Fig. 4c 4d). Moreover, there were not significant changes for solution color of the Rh-OH and Cu^{2+} mixture in the presence of EDTA. These results indicated that the responses of Rh-OH to Cu^{2+} were irreversible in neutral solution, similar to that in acidic condition reported previously [31]. Additionally, S^{2-} was used to further verify the reversibility of SRh-OH with Cu^{2+} (Fig. S4). The red fluorescence of SRh-OH with Cu^{2+} would be faint upon addition excess of S^{2-}. The mixture of SRh-OH and Cu^{2+} might be used as a "turn-off" fluorescent probe for S^{2-} monitoring.

3.6. Kinetic analysis and Job's plot of SRh-OH towards Cu^{2+}

In order to illuminate the difference between SRh-OH and Rh-OH with Cu^{2+}, the time-course of SRh-OH and Rh-OH with Cu^{2+} was shown in Fig. 5a. In the absence of Cu^{2+}, the emission intensity of SRh-OH and Rh-OH solution was faint and constant. When 5 equiv. Cu^{2+} was added, the emission intensity of Rh-OH (593 nm) increased slowly and was still weak after 60 s. Upon further addition of 10 equiv. Cu^{2+} into Rh-OH, there were the same growth trend and similar emission intensity within the same time. Unlike Rh-OH, SRh-OH showed distinct emission intensity and short response time in the presence of low Cu^{2+} concentration. Even in the presence of 0.5 equiv. Cu^{2+}, the fluorescence intensity at 593 nm of SRh-OH can achieve the maximum within 20 s. Though the concentration of Cu^{2+} was 10 times lower than Rh-OH, the

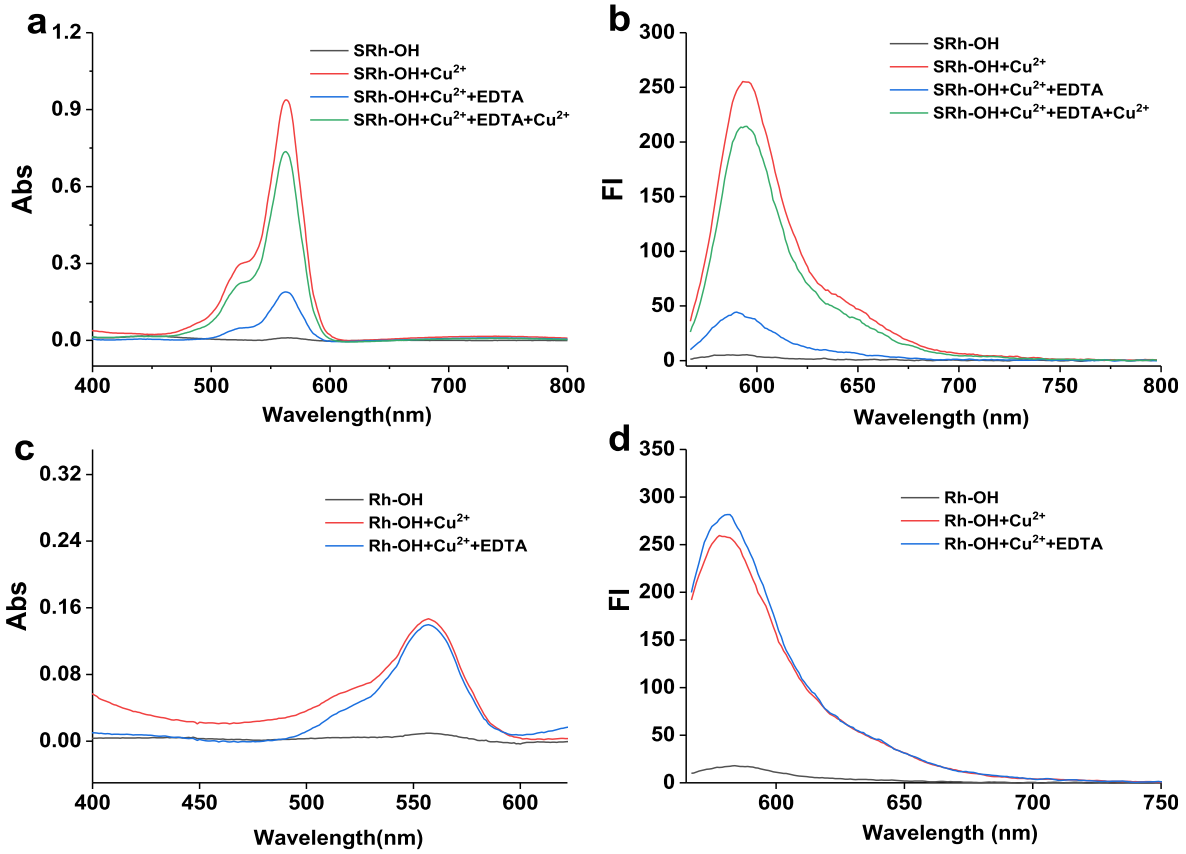

Fig. 4. Spectral changes of SRh-OH (a-b) (2×10^{-5} M) and Rh-OH (c-d) in CH_3CN/HEPES (4/6, v/v; 20 mM HEPES buffer; pH 7.4) upon successive addition of Cu^{2+} and EDTA.

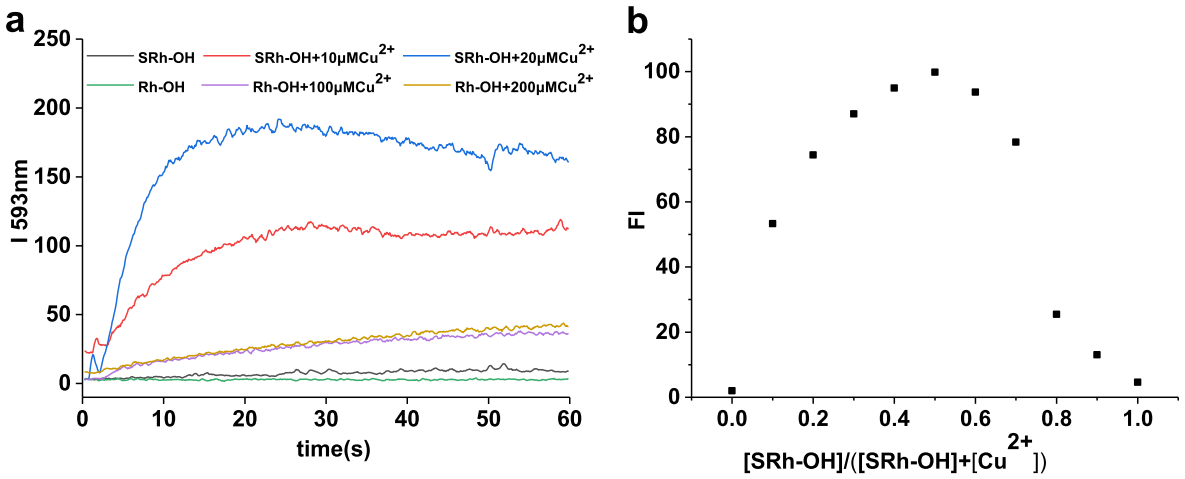

Fig. 5. Kinetic detection (a) and Job's plot (b) of SRh-OH and Rh-OH.

fluorescence intensity of SRh-OH was more than 3 times that of Rh-OH within the same time. Meanwhile, the stoichiometry of the SRh-OH with Cu^{2+} was 1:1, determined by Job's plot (Fig. 5b). According to above results, a reversible binding mode of SRh-OH with Cu^{2+} was proposed in Scheme 2.

3.7. Cu^{2+} fluorescent image in Hela cells

Owing to higher sensitivity of SRh-OH to Cu^{2+}, probe SRh-OH was used to map Cu^{2+} distribution in Hela cells. Red fluorescence could be invisible in Hela cells incubated with SRh-OH (5 μM) for 10 min (Fig. 6a). Upon addition of Cu^{2+} (50 μM), the fluorescence of Hela cells stained with SRh-OH enhanced significantly. To further investigate the target accumulation of SRh-OH in Hela cells, co-localization experiments were tested, as shown in Fig. 6b, 6c. Hela cells were stained with SRh-OH and Rh123 (3,6-diamino-9-[2-(methoxy-carbonyl) phenyl]-xanthylium chloride), a mitochondrial tracker. After 50 μM Cu^{2+} was added, there was strong red and green fluorescence in Ch1 and Ch2 of Hela cells, respectively (Fig. 6b). The merged image overlaid very well, and its Pearson's coefficient was up to 0.91. Intensity profile of linear ROI across Hela cells stained with SRh-OH and Rh123 varied in close synchrony (Fig. 6b). Additionally, it was easily found that probe SRh-OH seemed to be directionally accumulated not only in mitochondria but also in some other organelles in which strong fluorescent spots emitted. To further demonstrate the dot organells, co-localization experiments were performed by co-staining Hela cells with LysoTracker Green DND-26. As illustrated in Fig. 6c, in Ch1 Hela cells stained with SRh-OH exhibited strong red fluorescent spots which overlaid well with the fluorescence of Hela cells stained with DND-26 in Ch2. These results indicated that SRh-OH could not only accumulate in mitochondria for Cu^{2+} image, but also map the Cu^{2+} distribution in lysosomes of Hela cells. Additionally, the cytotoxicity of SRh-OH was evaluated by using MTT assay (Fig. S5). When Hela cells were treated with SRh-OH (0–10 μM) for 12 h, the cell viabilities were higher than 92%, suggested low cytotoxicity of SRh-OH (5 μM). After Hela cells stained with 5 μM SRh-OH were further incubated with 50 μM Cu^{2+} for 5 min, the cell viability did not show much more difference.

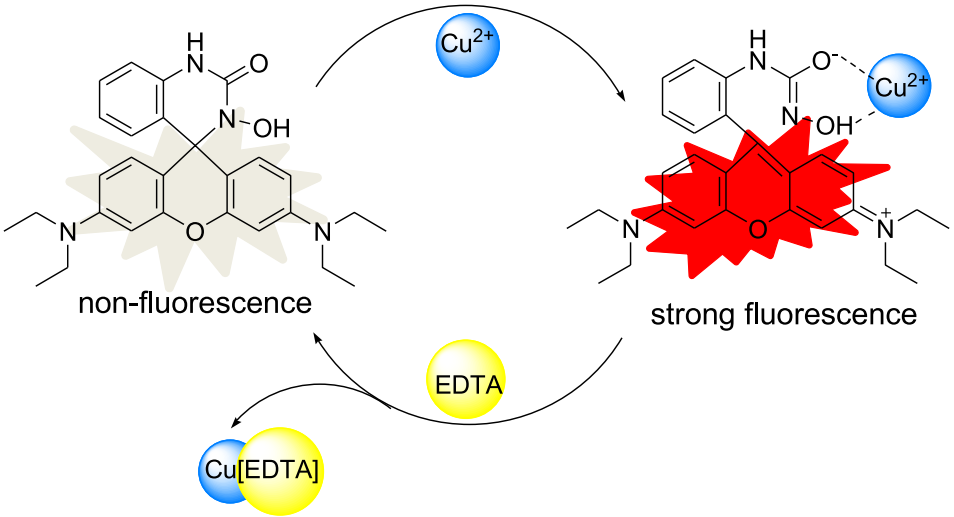

Scheme 2. Proposed binding mode of SRh-OH with Cu^{2+}.

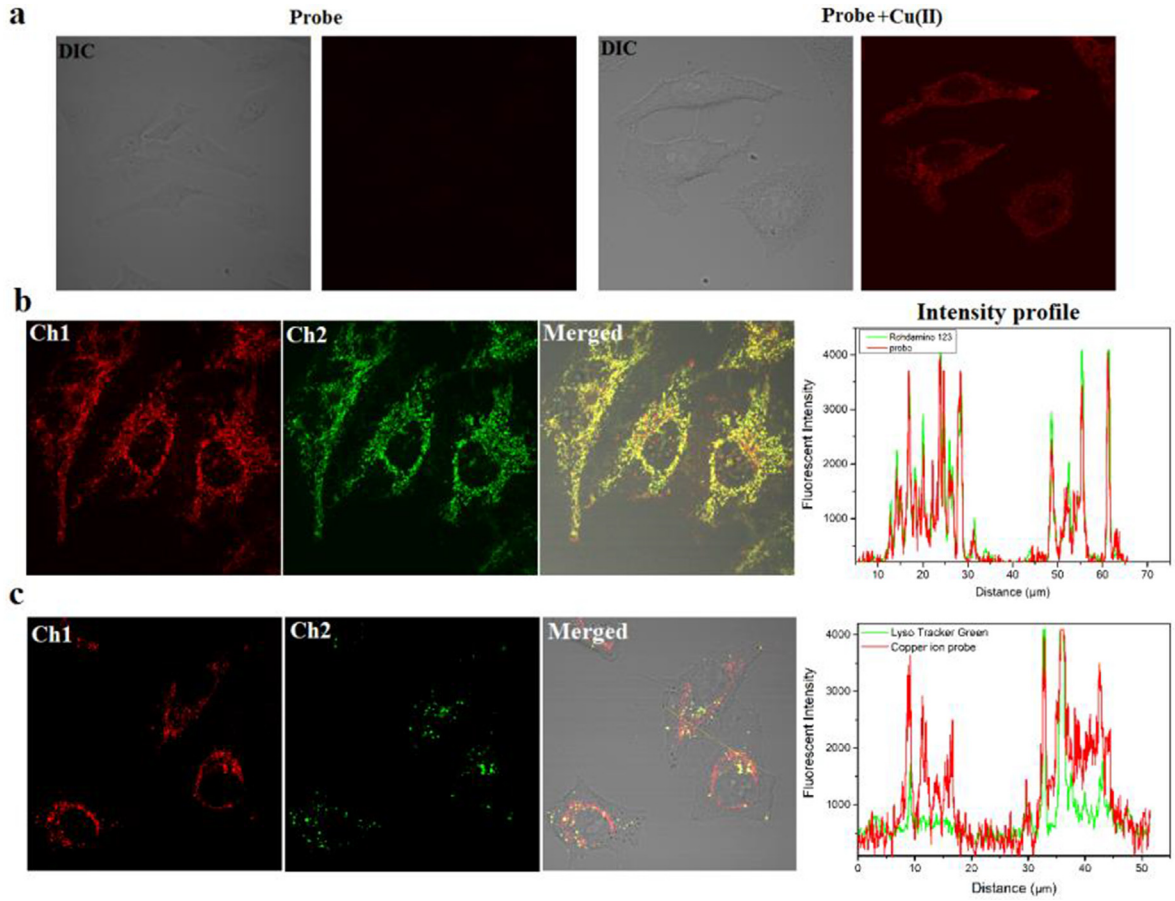

Fig. 6. (a) DIC and Fluorescent images of Hela cells stained with SRh-OH (5 μM) in the absence and presence of Cu^{2+} (50 μM). (b) Co-localization fluorescent image of Hela stained with SRh-OH and Rh123 in the presence of Cu^{2+} (50 μM), (c) Co-localization fluorescent image of Hela stained with SRh-OH and Lyso Tracker Green in the presence of Cu^{2+} (50 μM). From left to right: Ch1: Ex 559 nm, Em 565–665 nm, Ch2: Ex 488 nm, Em 495–535 nm, Merged of DIC, Ch1 and Ch2, Intensity profile of region of interest. (For interpretation of the references to color in this figure legend, the reader is referred to the web version of this article.)

4. Conclusion

In summary, we developed a general synthetic route to synthesize a new six-membered spiro-rhodamine probe (SRh-OH) bearing urea structure for Cu^{2+}. Compared with five-membered spiro-rhodamine (Rh-OH), SRh-OH exhibited higher selectivity and sensitivity of spectral responses to Cu^{2+}. Upon addition of 10 equiv. Cu^{2+}, there was a significant absorption peak at 563 nm of SRh-OH and its molar extinction coefficient was as high as 4.73×10^4 $Lmol^{-1}cm^{-1}$, which would be sensitive for Cu^{2+} detection with naked eyes. The titration curve showed that there was a linear relationship between SRh-OH and Cu^{2+}in the concentration range from 0 to 28 μM (R^2 = 0.988). Meanwhile, there was 17-folds enhancement of fluorescence of SRh-OH upon addition of 28 μM Cu^{2+}. Calculated by the ratio of signal to noise(S/N = 3), the detection limit of SRh-OH was 26 nM, which was lower than that of Rh-OH. Determined by Job's plot, the stoichiometry of the SRh-OH with Cu^{2+} was 1:1. The reversible binding mode of SRh-OH with Cu^{2+} was further confirmed and propsed by EDTA and S^{2-} addition. Finally, SRh-OH can map the distribution of Cu^{2+} not only in mitochondria but also in lysosomes of live Hela cells.

CRediT authorship contribution statement

Yongsheng Lei: Investigation, Validation, Writing – original draft. **Yannan Xiao:** Investigation. **Lin Yuan:** Investigation. **Chen Ma:** Investigation. **Haibo Yu:** Conceptualization, Methodology, Investigation, Writing – review & editing. **Xinfu Zhang:** Resources, Supervision, Validation. **Ying Zhang:** Resources, Supervision, Validation. **Yi Xiao:** Resources, Supervision, Validation.

Declaration of Competing Interest

The authors declare that they have no known competing financial interests or personal relationships that could have appeared to influence the work reported in this paper.

Acknowledgment

This work was supported by the grants from Liaoning Revitalization Talents Program (XLYC1907002), Shenyang Young and Middle-aged Innovators Program (RC200569), Open Research Fund from State Key Laboratory of Fine Chemicals (KF1906), Program of Liaoning Province Education Administration (LJC201911), Joint Research Fund Liaoning- Shenyang National Laboratory for Materials Science (20180510044) and Liaoning University Students' Innovation and Entrepreneurship Training Program.

Appendix A. Supplementary material

Supplementary data to this article can be found online at https://doi.org/10.1016/j.saa.2022.121334.

References

[1] H.N. Kim, M.H. Lee, H.J. Kim, et al., A new trend in rhodamine-based chemosensors: application of spirolactam ring-opening to sensing ions, Chem. Soc. Rev. 37 (2008) 1465–1472, https://doi.org/10.1039/B802497A.

[2] X. Chen, T. Pradhan, F. Wang, J.S. Kim, J. Yoon, Fluorescent chemosensors based on spiroring-opening of xanthenes and related derivatives, Chem. Rev. 112 (3) (2012) 1910–1956, https://doi.org/10.1021/cr200201z.

[3] Y. Yang, Q. Zhao, W. Feng, F. Li, Luminescent Chemodosimeters for Bioimaging, Chem. Rev. 113 (1) (2013) 192–270, https://doi.org/10.1021/cr2004103.

[4] L.D. Lavis, Teaching Old Dyes New Tricks: Biological Probes Built from Fluoresceins and Rhodamines, Annu. Rev. Biochem. 86 (2017) 825–843, https://doi.org/10.1146/annurev-biochem-061516-044839.

[5] L.e. Ju, W. Gao, J. Zhang, T. Qin, Z. Du, L. Sheng, S.-A. Zhang, A new absorption/fluorescence dual-mode hydrochromic dye for water-jet printing and anti-counterfeiting applications, J. Mater. Chem. C. 8 (8) (2020) 2806–2811, https://doi.org/10.1039/C9TC06522A.

[6] Z. Du, J. Liu, H. Gai, L. Sheng, S.-A. Zhang, A high-performance visible laser rewritable black paper, J. Mater. Chem. C. 8 (34) (2020) 11675–11680, https://doi.org/10.1039/D0TC02241A.

[7] X. Hu, Y. Li, T. Liu, G. Zhang, S. Liu, Intracellular Cascade FRET for Temperature Imaging of Living Cells with Polymeric Ratiometric Fluorescent Thermometers, ACS Appl. Mater. Interfaces 7 (28) (2015) 15551–15560, https://doi.org/10.1021/acsami.5b04025.

[8] L. Meng, S. Jiang, M. Song, F. Yan, W. Zhang, B. Xu, W. Tian, TICT-Based Near-Infrared Ratiometric Organic Fluorescent Thermometer for Intracellular Temperature Sensing, ACS Appl. Mater. Interfaces 12 (24) (2020) 26842–26851, https://doi.org/10.1021/acsami.0c03714.

[9] V. Vishnuvardhan, R. Kala, T. Prasada Rao, Chemical switch based reusable dual optoelectronic sensor for nitrite, Anal. Chim. Acta 623 (1) (2008) 53–58, https://doi.org/10.1016/j.aca.2008.05.075.

[10] A. Diac, M. Focsan, C. Socaci, A.-M. Gabudean, C. Farcau, D. Maniu, E. Vasile, A. Terec, L.M. Veca, S. Astilean, Covalent conjugation of carbon dots with Rhodamine B and assessment of their photophysical properties, RSC Adv. 5 (95) (2015) 77662–77669, https://doi.org/10.1039/C5RA13161H.

[11] Z. Ye, H. Yu, W. Yang, et al., Strategy to Lengthen the On-Time of Photochromic Rhodamine Spirolactam for Super-resolution Photoactivated Localization Microscopy, J. Am. Chem. Soc. 141 (2019) 6527–6536, https://doi.org/10.1021/jacs.8b11369.

[12] J. Fölling, V. Belov, R. Kunetsky, R. Medda, A. Schönle, A. Egner, C. Eggeling, M. Bossi, S.W. Hell, Photochromic Rhodamines Provide Nanoscopy with Optical Sectioning, Angew. Chem. Int. Edit. 119 (33) (2007) 6382–6386.

[13] K. Kolmakov, V.N. Belov, C.A. Wurm, B. Harke, M. Leutenegger, C. Eggeling, S.W. Hell, A Versatile Route to Red-Emitting Carbopyronine Dyes for Optical Microscopy and Nanoscopy, Eur. J. Org. Chem. 2010 (19) (2010) 3593–3610, https://doi.org/10.1002/ejoc.201000343.

[14] V. Dujols, F. Ford, A.W. Czarnik, A Long-Wavelength Fluorescent Chemodosimeter Selective for Cu(II) Ion in Water, J. Am. Chem. Soc. 119 (31) (1997) 7386–7387, https://doi.org/10.1021/ja971221g.

[15] J.S. Wu, I.C. Hwang, K.S. Kim, et al., Rhodamine-Based Hg2+-Selective Chemodosimeter in Aqueous Solution: Fluorescent OFF−ON, Org. Lett. 9 (2007) 907–910, https://doi.org/10.1021/ol070109c.

[16] Y. Xia, X. Liu, D. Wang, Z. Wang, Q. Liu, H. Yu, M. Zhang, Y. Song, A fluorometric and mitochondrion-targetable probe for rapid, naked-eye test of hypochlorite in real samples, Chinese Chem. Lett. 29 (10) (2018) 1517–1520, https://doi.org/10.1016/j.cclet.2018.01.054.

[17] H. Yu, G. Li, B. Zhang, X. Zhang, Y. Xiao, J. Wang, Y. Song, A neutral pH probe of rhodamine derivatives inspired by effect of hydrogen bond on pKa and its organelle-targetable fluorescent imaging, Dyes Pigments 133 (2016) 93–99, https://doi.org/10.1016/j.dyepig.2016.05.028.

[18] Y.u. Xiang, A. Tong, P. Jin, Y. Ju, New Fluorescent Rhodamine Hydrazone Chemosensor for Cu(II) with High Selectivity and Sensitivity, Org. Lett. 8 (13) (2006) 2863–2866, https://doi.org/10.1021/ol0610340.

[19] J.Y. Kwon, Y.J. Jang, Y.J. Lee, et al., A Highly Selective Fluorescent Chemosensor for Pb2+, J. Am. Chem. Soc. 127 (2005) 10107–10111, https://doi.org/10.1021/ja051075b.

[20] M. Beija, C.A. Afonso, J.M. Martinho, Synthesis and applications of Rhodamine derivatives as fluorescent probes, Chem. Soc. Rev. 38 (2009) 2410–2433, https://doi.org/10.1039/b901612k.

[21] E. Tomat, S.J. Lippard, Ratiometric and intensity-based zinc sensors built on rhodol and rhodamine platforms, Inorg. Chem. 49 (20) (2010) 9113–9115, https://doi.org/10.1021/ic101513a.

[22] Y.-Q. Sun, J. Liu, X. Lv, Y. Liu, Y. Zhao, W. Guo, Rhodamine-inspired far-red to near-infrared dyes and their application as fluorescence probes, Angew. Chem. Int. Edit. 51 (31) (2012) 7634–7636, https://doi.org/10.1002/anie.201202264.

[23] Y. Wei, Z. Aydin, Y.i. Zhang, Z. Liu, M. Guo, A turn-on fluorescent sensor for imaging labile Fe(3+) in live neuronal cells at subcellular resolution, Chembiochem. 13 (11) (2012) 1569–1573.

[24] B. Biswal, D. Mallick, B. Bag, Signaling preferences of substituted pyrrole coupled six-membered rhodamine spirocyclic probes for Hg2+ ion detection, Org. Biomol. Chem. 14 (7) (2016) 2241–2248, https://doi.org/10.1039/C5OB02606G.

[25] B. Wang, X. Cui, Z. Zhang, et al., A six-membered-ring incorporated Si-rhodamine for imaging of copper (ii) in lysosomes, Org. Biomol. Chem. 14 (2016) 6720–6728, https://doi.org/10.1039/c6ob00894a.

[26] K. Huang, D. Han, X. Li, et al., A new Cu2+-selective fluorescent probe with six-membered spirocyclic hydrazide and its application in cell imaging, Dyes. Pigments. 171 (2019), https://doi.org/10.1016/j.dyepig.2019.107701 107701.

[27] A. Majumdar, C.S. Lim, H.M. Kim, et al., New six-membered pH-insensitive rhodamine spirocycle in selective sensing of Cu2+ through C-C bond cleavage and its application in cell imaging, ACS Omega 2 (2017) 8167–8176, https://doi.org/10.1021/acsomega.7b01324.

[28] C. Wu, Q.N. Bian, B.G. Zhang, et al., Ring expansion of spiro-thiolactam in rhodamine scaffold: switching the recognition preference by adding one atom, Org. Lett. 14 (2012) 4198–4201, https://doi.org/10.1021/ol3018598.

[29] L.-L. Yang, A.-L. Tang, P.-Y. Wang, S. Yang, Switching of C-C and C–N Coupling/Cleavage for Hypersensitive Detection of Cu2+ by a Catalytically Mediated 2-Aminoimidazolyl-Tailored Six-Membered Rhodamine Probe, Org. Lett. 22 (21) (2020) 8234–8239, https://doi.org/10.1021/acs.orglett.0c02814.

[30] Z. Wang, Q. Zhang, J. Liu, R. Sui, Y. Li, Y. Li, X. Zhang, H. Yu, K. Jing, M. Zhang, Y. Xiao, A twist six-membered rhodamine-based fluorescent probe for hypochlorite detection in water and lysosomes of living cells, Anal. Chim. Acta 1082 (2019) 116–125, https://doi.org/10.1016/j.aca.2019.07.046.

[31] X. Chen, J. Jia, H. Ma, S. Wang, X. Wang, Characterization of rhodamine B hydroxylamide as a highly selective and sensitive fluorescence probe for copper(II), Anal. Chim. Acta 632 (1) (2009) 9–14, https://doi.org/10.1016/j.aca.2007.08.025.

[32] G.L. Long, J.D. Winefordner, Limit of Detection A Closer Look at the IUPAC Definition, Anal. Chem. 55 (07) (1983) 712A–724A, https://doi.org/10.1021/ac00258a724.